Systematic extension of the length of the organic conjugated π-system of mesoporous silica-based organic–inorganic hybrid materials†

Maximilian Cornelius,[a] Frank Hoffmann,[b] Boris Ufer,[c] Peter Behrens[c] and Michael Fröba*[b]

The first systematic investigations on the optical properties of mesoporous silica-based organic–inorganic hybrid materials is reported. It could be shown that the optical absorption properties of the incorporated organic functionalities are tuneable by adjusting the length of the conjugation of the π-electron systems or by integration of heteroatoms therein. For this purpose, two new bis-silylated compounds with 18 π-electron systems, namely 4,4′-bis((E)-2-(triethoxysilyl)vinyl)stilbene and 1,2-bis(4-((E)-2-(triethoxysilyl)vinyl)phenyl)diazene and their related mesoporous hybrid materials, were synthesised. On the basis of solid state UV-vis absorption spectra it is demonstrated that for highly conjugated and elongated organic bridges the absorption maximum reaches the visible region resulting in a yellow powder for a pure hydrocarbon backbone and a deep red powder for an azobenzene containing material.

Introduction

Since the discovery of mesoporous materials in the early 1990s by researchers of the Mobil Oil Company the scientific results within this field of porous materials have expanded rapidly.[1,2] With the utilisation of supramolecular structure directing agents (SDAs) formed by amphiphilic molecules, inorganic mesoporous materials became widely available. At first, these preparation routes were applied in the synthesis of mesoporous pure silica materials. As a logical consequence of these promising results different research groups tried to transfer this procedure to silsesquioxanes, *i.e.* molecular precursors which were already well known from sol–gel chemistry. The resulting organic–inorganic hybrid materials should combine the major advantages of pure inorganic materials like for instance thermal stability with the variety of potential organic functionalisations within one homogeneous material by offering a high specific surface area at the same time. In 1999 a major breakthrough was achieved independently by three working groups who succeeded in preparing a silica-based ordered mesoporous organic–inorganic hybrid material, *i.e.* periodic mesoporous organosilica (PMO).[3–5] Up to now a variety of functional organic groups, which are genuine integral part of the pore walls, *i.e.* are covalently bonded on both ends to the silica matrix, could be successfully incorporated within these materials, among them, for instance, aliphatic, aromatic,

heteroaromatic or saturated dendrimer-like moieties.[6] Depending on the employed SDA and the reaction parameters like temperature or pH value the mesopores can be adjusted within a certain range. Furthermore these settings determine the pore structure of the material, like hexagonal, cubic or lamellar. One special and unique feature of these PMOs, which can not be found in pure silica materials, is a crystal-like pore wall structure.[7–12] The origin of these crystal-like arrangement of the organic bridges is not yet fully understood but due to the fact that this behaviour is only observed for rigid unsaturated or aromatic compounds, *i.e.* molecules with π-electron systems, it is most likely that this assembly is the result of a π-stacking effect.

Recently, Sayari and Wang[13] and Cornelius *et al.*[14] prepared a novel PMO material with a fully conjugated 10 π-electron system as an organic bridge which exceeds the benzene ring. This was accomplished by synthesising the corresponding precursor *via* a Pd-catalysed double Heck coupling of 1,4-dibromobenzene with vinyltriethoxysilane. As was pointed out in our previous paper[14] this was only regarded as a starting point for new PMOs with extended π-systems. Consequently, following this approach, we present here not only two new organic–inorganic hybrid materials with organic units comprising 18 fully conjugated π-electrons, thereby reaching the optical absorption region of mesoporous hybrid materials as will be shown below, but we also report for the first time on the systematic investigation of the optical properties of such silica-based mesoporous hybrid materials with π-systems in general. In particular the field of organic–inorganic hybrid materials with special or unique optical properties, for instance luminescence features,[15,16] is a new and interesting topic.

In order to gain deeper insights into the way in which the optical properties depend on the length of the (conjugated) π-system we investigated the following five mesoporous organic–inorganic hybrid materials with increasing numbers of π-electrons (the first three materials are already known from the established stock of PMOs): ethene-bridged (**1**, 2 π-electrons),

[a]Institute of Inorganic and Analytical Chemistry, Justus Liebig University Giessen, Heinrich-Buff-Ring 58, D-35392 Giessen, Germany

[b]Institute of Inorganic and Applied Chemistry, University of Hamburg, Martin-Luther-King-Platz 6, D-20146 Hamburg, Germany. E-mail: michael.froeba@chemie.uni-hamburg.de; Fax: +49 40 428 38 6348; Tel: +49 40 428 38 3137

[c]Institute of Inorganic Chemistry, Leibniz University Hannover, Callinstr. 9, D-30167 Hannover, Germany

† Electronic supplementary information (ESI) available: Characterisation of the new organosilane precursors as well as ethene-, benzene- and 1,4-divinylbenzene-bridged PMOs. See DOI: 10.1039/b801034j
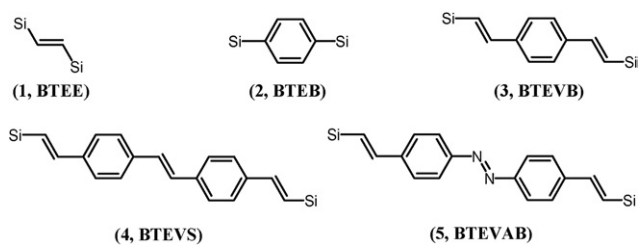
This journal is © The Royal Society of Chemistry 2008

J. Mater. Chem., 2008, **18**, 2587–2592 | 2587

Fig. 1 Structural formulae and abbreviations of the organic bridges of the mesoporous organic–inorganic hybrid materials, from which the optical properties were investigated in this publication (Si = Si(OEt)$_3$).

benzene-bridged (**2**, 6 π-electrons), 1,4-divinylbenzene-bridged (**3**, 10 π-electrons), 4,4′-divinylstilbene-bridged (**4**, 18 π-electrons), and 4,4′-divinylazobenzene-bridged (**5**, 18 π-electrons) hybrid material samples (for structural formulae see Fig. 1)

Since PMOs are regarded as promising materials for various applications in the fields of chromatography, separation, fabrication of low-k devices, immobilisation of bio-molecules and catalysis, this work can also be regarded as a first step in order to open up a new field of potential applications due to their tuneable optical properties.

Experimental

Syntheses

All syntheses were carried out in vacuum-dried glass vessels with purified and dry solvents under argon atmosphere using Schlenk techniques. The chemicals were purchased from Sigma-Aldrich, Fluka and ABCR and were used without further purification.

Precursor syntheses. The precursors **1–3** were synthesised according to standard literature procedures.[14,17,18]

The synthesis of the new (pure hydrocarbon) organosilane precursor (**4**) was accomplished *via* a two-step synthesis with (*E*)-4,4′-dibromostilbene as an intermediate.[19] In the second step a palladium-catalysed double Heck coupling of (*E*)-4,4′-dibromostilbene with vinyltriethoxysilane was carried out. In a typical synthesis 15.02 g (0.044 mol) of (*E*)-4,4′-dibromostilbene was added to 250 ml dimethylformamide in a 500 ml three-necked flask. To this mixture 15 ml (0.11 mol) triethylamine, 25 ml (0.12 mol) vinyltriethoxysilane and 0.148 g (1.28 × 10^{-4} mol) of tetrakis(triphenylphosphine)palladium(0) were added. The educt dissolved completely during heating to 120 °C. After stirring the reaction mixture for 4 d at this temperature the resulting solution was cooled to 0 °C to complete the precipitation of the formed salt (HNEt$_3$Br). After removal of the salt by filtration the solvent was removed under reduced pressure. The residue was taken up in 150 ml CCl$_4$ and the mixture was filtered again. The solvent was again removed and the resulting brown oil was taken up in 100 ml Et$_2$O. After filtration the brownish solution was concentrated. The obtained raw product (light brown oil) was purified by a twofold kugelrohr distillation under high vacuum. 15.3 g (0.027 mol, yield: 61%) of the organosilane precursor were obtained as a light yellow solid (solidification occurred after cooling to room temperature). The product was characterised by ^{1}H and ^{13}C NMR measurements and IR spectroscopy (for details see ESI,† Fig. S1–S3).

The synthesis of the new precursor with the diazene group (**5**) was carried out in two steps with (*E*)-4,4′-dibromoazobenzene as the intermediate,[20] followed by a Heck coupling with vinyltriethoxysilane. In a typical synthesis 10.0 g (0.029 mol) (*E*)-4,4′-dibromoazobenzene were mixed in approx. 120 ml dimethylformamide in a 250 ml three-necked flask. To this mixture 20 ml (0.096 mol) of vinyltriethoxysilane and 20 ml (0.144 mol) triethylamine as well as 100 mg (8.6 × 10^{-4} mol) tetrakis(triphenylphosphine)palladium(0) were added. Afterwards, this deep red-brown mixture was heated to 115 °C whereas the educt was dissolved completely. After stirring the reaction mixture for 4 d at this temperature the resulting solution was cooled to 0 °C to complete the precipitation of the formed salt (HNEt$_3$Br). After removal of the salt by filtration the solvent and surplus liquid educts were removed under reduced pressure. The residue was taken up in toluene and the insoluble solid was removed by filtration. The filtrate was concentrated under reduced pressure. The residue was extracted by Soxhlet extraction with *n*-hexane. After removal of the solvent a red oil was obtained: 10.2 g (0.018 mol, yield: 62%). The product was characterised by ^{1}H and ^{13}C NMR measurements and IR spectroscopy (for details see ESI,† Fig. S4–S6).

Syntheses of the hybrid materials. In a typical synthesis for the 4,4′-divinylstilbene-bridged hybrid material 0.69 g (1.9 × 10^{-3} mol) of octadecyltrimethylammonium chloride (OTAC) was dissolved under vigorous stirring in a solution of 0.08 g (2.0 × 10^{-3} mol) NaOH in 20 ml distilled water. Afterwards, a solution of 0.75 g (1.3 × 10^{-3} mol) BTEVS in 2 ml THF was added in order to adjust the molar ratio of the reaction mixture to BTEVS 1 : OTAC 1.47 : NaOH 1.48 : H$_2$O 824. The suspension was stirred at room temperature for 24 h followed by a hydrothermal treatment in a closed PE autoclave at 95 °C for 24 h. After filtration the as-synthesised composite material was obtained as a yellow powder which was washed three times with 200 ml of distilled water. The surfactant was removed by Soxhlet extraction with ethanol/HCl (conc.) (100 : 3, v/v) for 8 h.

In a typical synthesis for the 4,4′-divinylazobenzene-bridged hybrid material 0.366 g (1.05 × 10^{-3} mol) of OTAC was dissolved under vigorous stirring in a solution of 0.253 g (6.3 × 10^{-3} mol) NaOH in 20 ml distilled water. Afterwards this solution was added to 0.4 g (7.15 × 10^{-4} mol) BTEVAB in order to adjust the molar ratio of the reaction mixture to BTEVAB 1 : OTAC 1.47 : NaOH 8.84 : H$_2$O 1552. The suspension was stirred at room temperature for 24 h followed by a hydrothermal treatment in a closed PE autoclave at 95 °C for 24 h. After filtration the as-synthesised composite material was obtained as a red powder which was washed three times with 200 ml of distilled water. The surfactant was removed by Soxhlet extraction with ethanol–HCl (conc.) (100 : 3, v/v) for 8 h.

Characterisation

Powder X-Ray diffractograms were recorded at room temperature on a PANalytical X′Pert PRO instrument by applying filtered Cu-Kα radiation. The data in the SAXS region $2\theta < 10°$ were recorded with the following setup: 25 s step^{-1}; 0.0167° step size; 0.518° active length of the detector; divergence slit 1/32°. The data in the WAXS region $2\theta > 10°$ were recorded with the

following setup: 20 s step^{-1}; 0.0167° step size; 2.122° active 2θ range of the detector; fixed radiated length of 10 mm.

Transmission electron micrographs were obtained with a Philips C 30 microscope operating at 300 kV.

Nitrogen physisorption data were recorded on a Quantachrome Autosorb 6 instrument at 77 K. The BET surface areas were calculated from the adsorption branch in the range of $p/p° = 0.03–0.3$ while the BJH pore diameter distribution was determined from the desorption branch.

^{29}Si MAS NMR spectra were recorded with a 7 mm MAS system at a resonance frequency of 79.4 MHz using a Bruker MSL-400 spectrometer. The samples were spun at 3.5 kHz. Further experimental parameters were a $\pi/2$ pulse width of 6 ms, a recycle delay of 300 s and 1500 scans.

The UV-vis spectra of the precursors in n-hexane solution were recorded on an Agilent/HP-8453 spectrometer in the range from 200 to 800 nm. The solutions were diluted so that the absorbance was below 1. The UV-vis measurements of the hybrid materials were conducted in diffuse reflectance mode (Harrick or so-called Praying Mantis setup on a Varian Cary 5E spectrometer); BaSO$_4$ was used as white standard and dilutor. The obtained spectra were re-calculated to remission function $F(R)$ by applying the Kubelka–Munk theory in order to ensure that pure diffusive reflectivity values are obtained.[21]

Results and discussion

As ethene-, benzene-, and 1,4-divinylbenzene-bridged hybrid materials are already known in the literature and were synthesised according to the procedures described therein the characterisation (X-ray diffraction, N$_2$ physisorption) of these materials is only summarised in the ESI† (Fig. S7–S12).

4,4′-Divinylstilbene-bridged hybrid material

In Fig. 2 the powder X-ray diffractogram of the 4,4′-divinylstilbene-bridged hybrid material is shown.

This material reveals only one broad shoulder in the small angle region at $ca.$ 1.5° 2θ, indicating that almost no periodicity on the mesoscale is present. In addition four broad reflections, approximately at $2\theta = 4.8°$ ($d = 1.8$ nm), 9.6° (0.9 nm), 14.5° (0.6 nm) and 28.4° (0.3 nm), are observed. Note, due to the width
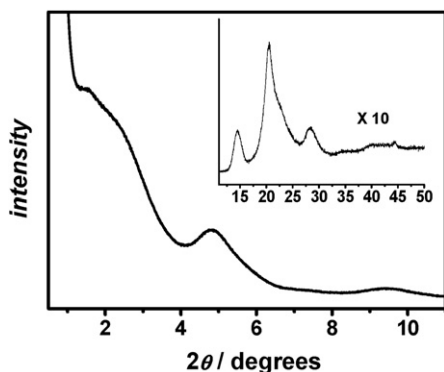
of these signals an accurate calculation of the corresponding d-values is not possible. The shapes as well as the low intensities of these signals suggest that these reflections are not caused by a strict crystal-like arrangement of the organic bridges but are rather results of (i) diffuse scattering processes meaning that intensity contributions will occur even if the Bragg condition is not fulfilled—this might be provoked by lattice planes that are not strictly parallel but show some modulations concerning their relative preferential orientation, and (ii) the circumstance that very short periodic assemblies of the organic spacers are present, which extend only over a few lattice planes so that even "non-crystalline regions" do not exclusively lead to destructive interference. In other words, even if the structure factor ($|F|^2$) is well defined, the convolution with the poor-defined lattice function ($\otimes |G|^2$) can be responsible for the reflection shifts compared to the expectation value, which would correspond exactly to the length of the organic spacer.

The occurrence of only one very broad shoulder in the small-angle region of the P-XRD diffractogram is supported by the transmission electron micrographs (see ESI,† Fig. S13), in which only a wormhole-like mesopore structure is observable but no mesoscale ordering. Nevertheless, it is clearly visible that the porosity extends over the whole hybrid material particles.

It is always useful to declare exactly the reasons which are responsible if the ordering process in the presence of the SDA failed, but a plausible explanation in this case could be the fact that **4** is solid and therefore has to be dissolved in an organic solvent prior to the hydrolysis and condensation step. This organic solvent is able to disturb the formation of a liquid crystal phase and therefore leads to non-periodic mesoporous hybrid materials.

The nitrogen physisorption measurement (Fig. 3) reveals an isotherm typical of mesoporous materials with a capillary condensation step at $p/p° = 0.7$. The mean pore diameter and the pore volume, as determined from the desorption branch by the BJH method, are 5.4 nm and 0.76×10^{-6} m^3 g^{-1}, respectively. The specific BET surface area amounts to 620 m^2 g^{-1}. A possible explanation for this high pore diameter value could be due the fact that the hydrophobicity of the precursor increases with the
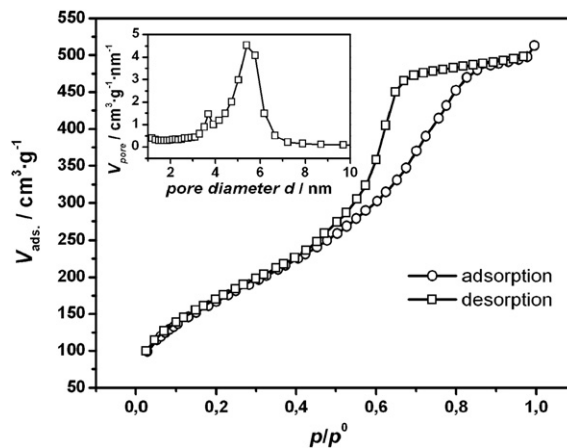

Fig. 2 P-XRD pattern of the mesoporous 4,4′-divinylstilbene-bridged hybrid material. Small angle region (large), wide angle region (inset).

Fig. 3 Nitrogen adsorption–desorption isotherms of the mesoporous 4,4′-divinylstilbene-bridged hybrid material and BJH pore size distribution (inset) measured at 77 K.
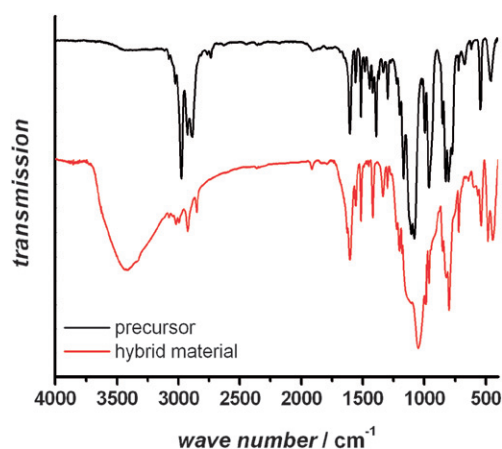
This journal is © The Royal Society of Chemistry 2008

J. Mater. Chem., 2008, **18**, 2587–2592 | 2589

Fig. 4 Comparison of the IR spectra of **4** (black, top) and the corresponding 4,4′-divinylstilbene-bridged hybrid material (red, bottom).

Fig. 5 P-XRD pattern of the mesoporous 4,4′-divinylazobenzene-bridged hybrid material. Small angle region (large), wide angle region (inset).

length of the organic bridge. At the same time the polarity of the precursor and of the structure directing agent are converging which causes a diffusion of the precursor into the inner part of the micelles as a result of "polarity matching". This process could then lead to a swollen micellar shape which yields an increased pore diameter within the hybrid material. Up to now this model is still hypothetical; further investigations covering the double role of the precursor as a swelling agent and as the framework material are currently taking place.

To investigate the status of the organic functionality within the hybrid material two complementary methods were applied: (i) IR spectroscopy and (ii) ^{29}Si MAS NMR measurement. Based on the results of the IR spectroscopic data (Fig. 4) it is possible to check the integrity of the organic moieties as such, however, it is not possible to inspect the status of the silicon–carbon bonds with the help of vibrational spectroscopy, as was demonstrated recently by Hoffmann *et al.*[22] In order to determine the covalent attachment of the organic spacers to the silica matrix solid state ^{29}Si MAS NMR measurements were carried out (see ESI,† Fig. S12). Therein only T^2 and T^3 (corresponding to C–Si (OSi)$_2$(OH) and C–Si(OSi)$_3$ respectively) signals but no Q^n signals (attributed to silicon atoms tetrahedral surrounded by oxygens) in the range < −90 ppm are visible, meaning that virtually no Si–C bond cleavage occurred during the synthesis procedure.

From the IR spectra of the hybrid material the following vibrational modes can be assigned: 798 cm^{-1} (breathing mode of the benzene ring); 1512 cm^{-1} (δ(C–H)$_{i.p.arom.}$); 1604 cm^{-1} (ν(C=C)$_{arom.}$); 1626 cm^{-1} (ν(C=C)$_{vinyl.}$); 3418 cm^{-1} (ν(O–H)). With the logical exception of the O–H band (caused by the silanol groups, which are formed during the hydrolysis process) all other bands are also detected in the non-hydrolysed precursor, clearly indicating the integrity of the organic moiety.

4,4′-Divinylazobenzene-bridged hybrid material

Fig. 5 shows the X-ray diffraction pattern of the 4,4′-divinyl-azobenzene-bridged hybrid material.

It shows neither a periodic arrangement of the mesopores nor a lamellar crystal-like pore wall structure. The broad reflections
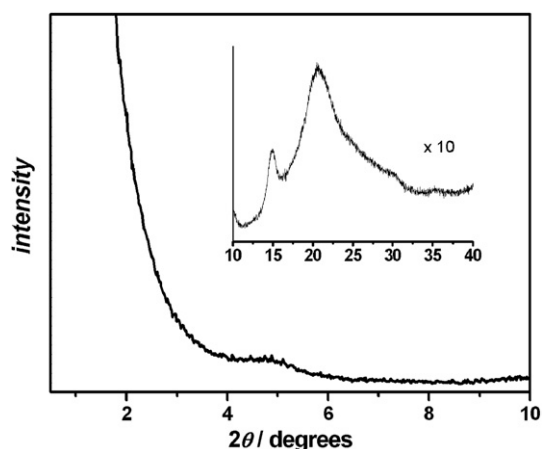
in the wide angle region are probably caused by very few ordered domains within almost X-ray amorphous particles.

In the TEM image of this sample only a wormhole-like mesophase with no preferential direction of the channels is observable (see ESI,† Fig. S14).

The nitrogen physisorption measurement shows a type IV isotherm with a capillary condensation step at $p/p°$ = 0.8 (Fig. 6). The mean pore diameter and the pore volume, as determined from the desorption branch by the BJH method, are 8.1 nm and 0.44×10^{-6} m^3 g^{-1}, respectively. The specific BET surface area is 240 m^2 g^{-1}. This unexpectedly high value for the pore diameter could be explained by the same processes taking place as in the case of the BTEVS related material (as mentioned above).

The IR spectra of **5** and the corresponding hybrid material are shown in Fig. 7. Due to the similarity of this organic moiety to the stilbene derivative almost the same vibrational modes are detectable and can be assigned as follows: 803 cm^{-1} (breathing mode of the benzene ring); 1513 cm^{-1} (δ(C–H)$_{i.p.arom.}$; 1600 cm^{-1} (ν(C=C)$_{arom.}$); 1629 cm^{-1} (ν(C=C)$_{vinyl.}$); 3422 cm^{-1} (ν(O–H)). Again, for the same reasons as mentioned above, it can be
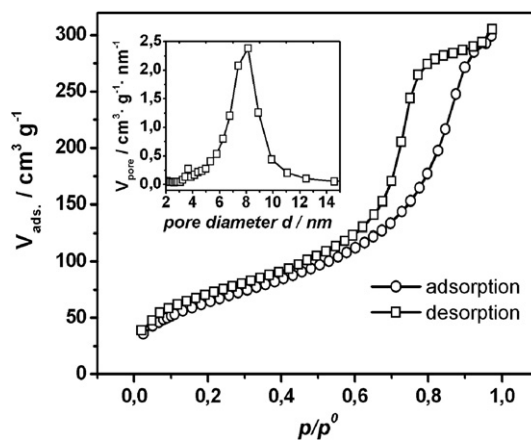

Fig. 6 Nitrogen adsorption–desorption isotherms of the mesoporous 4,4′-divinylazobenzene-bridged hybrid material and BJH pore size distribution (inset) measured at 77 K.
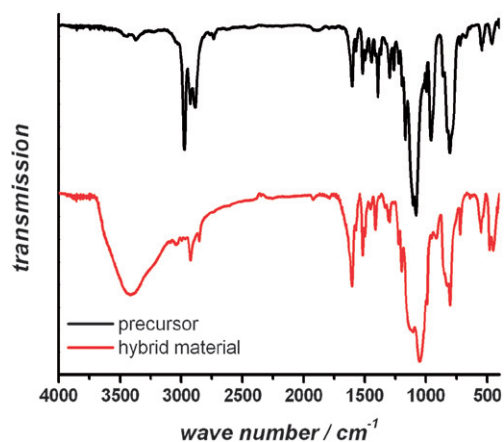
Fig. 7 Comparison of the IR spectra of **5** (black, top) and the corresponding 4,4′-divinylazobenzene-bridged hybrid material (red, bottom).

concluded that the organic group is preserved after the synthesis procedure.

UV-vis measurements

In order to investigate the optical properties UV-vis spectra of the precursors and of the corresponding mesoporous materials were recorded. The position of the centre of gravity of the band with the highest wavelengths corresponds to the energy of the HOMO–LUMO transition. However, in order to describe the optical signatures completely the indication of these positions is not sufficient. In this case, the highest wavelength where absorption occurs at all has also to be considered as this contributes to the overall colour impression of the sample. Therefore, we determined also the points where the absorption curve begins to rise (from the low-energy side).

The UV-vis spectra of the precursors (Fig. 8) reveal a clear and expected bathochromic shift with increasing length of the (conjugated) π-system. The π–π* transition of the ethene-bridged precursor should be located in the vacuum UV region, *i.e.* below 185 nm, but is not detectable with the applied
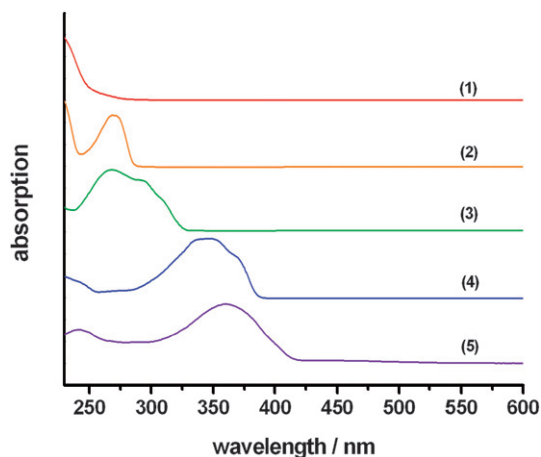

Fig. 8 Comparison of the UV-vis spectra of the organosilane precursors with various conjugated π-electron systems in *n*-hexane solution.
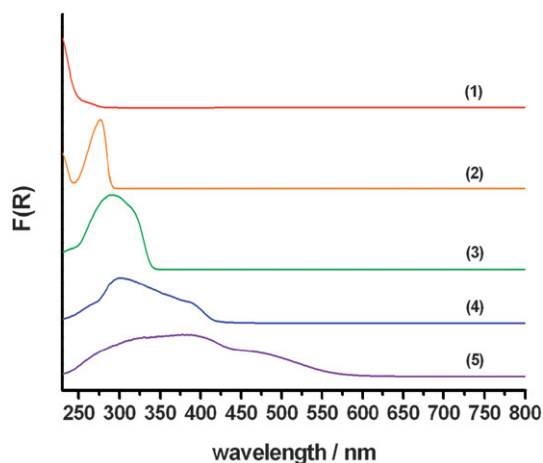

Fig. 9 Comparison of the UV-vis spectra of the organic–inorganic hybrid materials with various conjugated π-electron systems measured in reflectance mode, plotted as remission function *F*(*R*).

experimental setup. Furthermore, due to the increasing possibilities of electronic transitions in more extended π-systems the absorption bands become broader. The obtained spectra are in good agreement with the expected corresponding ones of the pure, un-silylated hydrocarbon compounds, which are well documented in the literature. A substitution of a hydrogen atom with a silicon containing moiety should result in a bathochromic shift of about +5 to +10 nm, due to the +*I* effect of silicon.

Note that in comparison to the precursor spectra the hybrid materials (Fig. 9) show a slight bathochromic shift of the absorption bands.

This shift is more pronounced for the 18 π-electron system (approx. +32 nm) and less for the shorter organic bridges (+8 nm). This effect may be attributed to π–π interactions between adjacent unsaturated organic bridges, which should be more intense for extended π-systems. For the 4,4′-divinyl-stilbene-bridged hybrid material the absorption reaches the visible region, which results in a pale yellow colour of the sample.

In the case of the azobenzene derivative the absorption occurs even within the green part of the visible spectrum due to a lower excitation energy for the *n*–π* transition, resulting in a deep-red colour of the material (see Fig. 10).
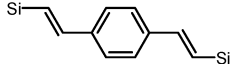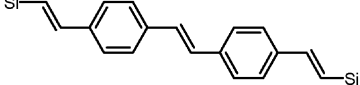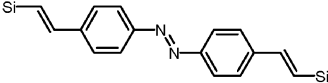
All hybrid materials show relatively broad absorption bands in their spectra. This broadening in comparison to the respective precursor spectra is more pronounced for the longer organic bridges and might be due to more extended vibronic couplings.

All structures of the precursors and the determined characteristic absorption wavelengths as well as those of the hybrid materials are summarised in Table 1.

Fig. 10 Photographs of the mesoporous hybrid materials with various conjugated π-electron systems: a) ethene-, b) benzene-, c) 1,4-divinyl-benzene-, d) 4,4′-divinylstilbene-, e) 4,4′-divinylazobenzene-bridged.

Table 1 Formulae and abbreviations of the precursors, the characteristic absorption wavelengths of the precursors and of the related hybrid materials

Precursor[a]/hybrid material[b]	Name	Precursor/nm	Hybrid material/nm
	BTEE	—	—
	BTEB	280	288
	BTEVB	325	340
	BTEVS	380	412
	BTEVAB	410	530

[a] Si = Si(OEt)$_3$. [b] Si = SiO$_{1.5}$.

Conclusions

By synthesising two completely new organosilane precursors, each consisting of a fully conjugated 18 π-electron system, an approach of extending the length of the organic bridge of organic–inorganic hybrid materials was successfully developed. Even though it was not possible to obtain real PMO materials from these extended precursors we were able to show for the first time that it is possible to obtain coloured mesoporous hybrid materials from one single bis-silylated silica source, which may open up new fields of applications, for instance those related to chemical sensing. In this sense the portfolio of such organic–inorganic hybrid materials was augmented considerably with the work at hand, showing that is possible to tune the optical properties, i.e. UV-vis absorption characteristics, by varying the length of conjugated π-systems of the organic bridges.

Acknowledgements

References

1 C. T. Kresge, M. E. Leonowicz, W. J. Roth, J. C. Vartuli and J. S. Beck, *Nature*, 1992, **359**, 710.
2 J. S. Beck, J. C. Vartuli, W. J. Roth, M. E. Leonowicz, C. T. Kresge, K. D. Schmitt, C. T.-W. Chu, D. H. Olson, E. W. Sheppard, S. B. McCullen, J. B. Higgins and J. L. Schlenker, *J. Am. Chem. Soc.*, 1992, **114**, 10834.
3 S. Inagaki, S. Guan, Y. Fukushima, T. Ohsuna and O. Terasaki, *J. Am. Chem. Soc.*, 1999, **121**, 9611.
4 B. J. Melde, B. T. Holland, C. F. Blanford and A. Stein, *Chem. Mater.*, 1999, **11**, 3302.
5 T. Asefa, M. J. MacLachlan, N. Coombs and G. A. Ozin, *Nature*, 1999, **402**, 867.
6 F. Hoffmann, M. Cornelius, J. Morell and M. Fröba, *Angew. Chem., Int. Ed.*, 2006, **45**, 3216.
7 S. Inagaki, S. Guan, Y. Fukushima, T. Ohsuna and O. Terasaki, *Nature*, 2002, **416**, 304.
8 M. P. Kapoor, Q. Yang and S. Inagaki, *J. Am. Chem. Soc.*, 2002, **124**, 15176.
9 N. Bion, P. Ferreira, A. Valente, I. S. Goncalves and J. Rocha, *J. Mater. Chem.*, 2003, **13**, 1910.
10 M. P. Kapoor, Q. Yang and S. Inagaki, *Chem. Mater.*, 2004, **16**, 1209.
11 Y. Yang and A. Sayari, *Chem. Mater.*, 2007, **19**, 4117.
12 Y. Xia and R. Mokaya, *J. Mater. Chem.*, 2006, **16**, 395.
13 A. Sayari and W. Wang, *J. Am. Chem. Soc.*, 2005, **127**, 12194.
14 M. Cornelius, F. Hoffmann and M. Fröba, *Chem. Mater.*, 2005, **17**, 6674.
15 P. Escribano, B. Julián-López, J. Planelles-Aragó, E. Cordoncillo, B. Viana and C. Sanchez, *J. Mater. Chem.*, 2008, **18**, 23.
16 C. Sanchez, B. Lebeau, F. Chaput and J.-P. Boilot, *Adv. Mater.*, 2003, **15**, 1969.
17 D. A. Loy, J. P. Carpenter, S. A. Yamanaka, M. D. McClain, J. Greaves, S. Hobson and K. J. Shea, *Chem. Mater.*, 1998, **10**, 4129.
18 R. J. P. Corriu, J. J. E. Moreau, P. Thepot and M. Wong Chi Man, *Chem. Mater.*, 1992, **4**, 1217.
19 K. S. Jeong, S. Y. Kim, U.-S. Shin, M. Kogej, N. T. M. Hai, P. Broekmann, N. Jeong, B. Kirchner, M. Reiher and C. A. Schalley, *J. Am. Chem. Soc.*, 2005, **127**, 17672.
20 O. H. Wheeler and D. Gonzales, *Tetrahedron Lett.*, 1964, **20**, 189.
21 P. Kubelka and F. Munk, *Z. Tech. Phys.*, 1931, **12**, 593.
22 F. Hoffmann, M. Güngerich, P. J. Klar and M. Fröba, *J. Phys. Chem. C*, 2007, **111**, 5648.